THE ASTROPHYSICAL JOURNAL, 343:672–677, 1989 August 15

IRAS 20460+1925: AN EXTREME SEYFERT 2 AND ONE OF THE MOST LUMINOUS GALAXIES KNOWN

JAY A. FROGEL
Ohio State University, Department of Astronomy; and Kitt Peak National Observatory, and National Optical Astronomy Observatories[1]
F. C. GILLETT
Kitt Peak National Observatory; and National Optical Astronomy Observatories
D. M. TERNDRUP
Cerro Tololo Inter-American Observatory, and National Optical Astronomy Observatories
AND
J. PATRICIA VADER
Yale University, Department of Astronomy
Received 1988 November 16; accepted 1989 February 1

ABSTRACT

IRAS 20460+1925 is identified with a Seyfert 2 galaxy at $z = 0.181$. It is dominated by an unresolved nucleus embedded in a region of extended emission with a diameter of 35 kpc. The bolometric luminosity of the galaxy is $7 \times 10^{12}\ L_{\odot}$ ($H_0 = 75$ km s^{-1} Mpc^{-1}), placing it second in luminosity among all known Seyfert 2 galaxies and all extragalactic objects discovered by *IRAS*. The full width half-maximum of forbidden and permitted lines is between 1700 and 2100 km s^{-1} in the rest frame. There is evidence for a permitted line component with twice this velocity width. There are no bright companion galaxies.

The 0.5–3.5 μm energy distribution of IRAS 20460+1925 is one of the reddest known for any type of galaxy while its 12–100 μm flux distribution is among the flattest known for an extragalactic source. There is no evidence for starlight in its spectrum. Energy distributions similar to that of IRAS 20460+1925 can be found in objects with a wide range in luminosity. Previous analyses of such objects lead us to conclude that reddened hot thermal and nonthermal emission from the nucleus itself dominates at shorter wavelengths while hot dust contributes to the longer wavelengths. The observed characteristics of IRAS 20460+1925 suggests that the nucleus of this galaxy would be more like a Seyfert 1 if it were not so heavily obscured by dust.

Subject headings: galaxies: individual (IRAS 20460+1925) — galaxies: photometry — galaxies: Seyfert

I. INTRODUCTION

Galaxies having flat far-infrared (FIR) colors frequently have Seyfert-like nuclei (e.g., de Grijp *et al.* 1985). After the serendipitous discovery of IRAS 00521−7054, a Seyfert 2 galaxy with exceptionally red 0.6–10 μm colors but one of the warmest (i.e., flattest) 12–100 μm energy distributions known for an extragalactic object (Frogel and Elias 1987), we realized that objects with flat FIR energy distributions—either galactic or extragalactic—were rare in the IRAS Point Source Catalog (IPSC) but appeared to include a disproportionate number of unusual cases. We searched the IPSC for objects that met the following criteria: $f_\nu(60)/f_\nu(100) \geq 1.0$, $4 \geq f_\nu(60)/f_\nu(25) \geq 1$, $|b| > 10°$, and high-quality detections at 25 and 60 μm. Upper limits at 100 μm were accepted provided that the upper limit was not greater than the 60 μm flux. Of the few hundred objects found many were planetary nebulae and a minority were previously known active galaxies. A list of $\sim$60 previously unidentified objects remained; for nearly all of these we have now obtained extensive optical and infrared data. Independent of our study, investigation of two sources on our list—the obscured active galaxy IRAS 23060+050 (Hill, Wynn-Williams, and Becklin 1987) and the luminous, tailed galaxy IRAS 05189−2524 (Sanders *et al.* 1988*a*)—confirmed that this small subset of the IPSC was indeed going to contain some unusual objects. Complete details of our study of the extragalactic sources on our list will be presented elsewhere (Vader *et al.* 1989).

IRAS 20460+1925 is the most interesting of the extragalactic objects on our final list. On the Palomar Observatory Sky Survey it appears moderately faint, stellar, and red; it lies in a crowded field at a galactic latitude of only −15°. From spectroscopic observations it is identified as an extreme Seyfert 2 at a redshift of 0.181. Bolometrically, it is the second most luminous object discovered by the *IRAS* survey as well as the second most luminous Seyfert 2 galaxy known after IRAS 09104+4109 (Kleinmann *et al.* 1988). Its near-infrared (NIR) energy distribution is one of the reddest known for a galaxy. In this paper we describe the properties of IRAS 2046+1925 and comment on its relevance for understanding the ultraluminous *IRAS* galaxies.

II. DATA AND ANALYSIS

a) Infrared Photometry

The position of IRAS 20460+1925 given in the IPSC was scanned at 2.2 μm with KPNO's 2.1 m telescope, an *f*/15 chopping secondary, and a single detector InSb system. A strong signal was found within 8″ of the *IRAS* position and coincident with the object marked on Figure 1 (Plate 27). Table 1 lists the *JHKLM* magnitudes and fluxes for this source measured on 1986 October 19. They have been put on the standard system of Elias *et al.* (1982). Within the uncertainties, *JHK* magnitudes measured with apertures of 6″ and 12″ diameter were identical. The *L* and *M* measurements were made only through

[1] Operated by the Association of Universities for Research in Astronomy, Inc., under contract with the National Science Foundation.

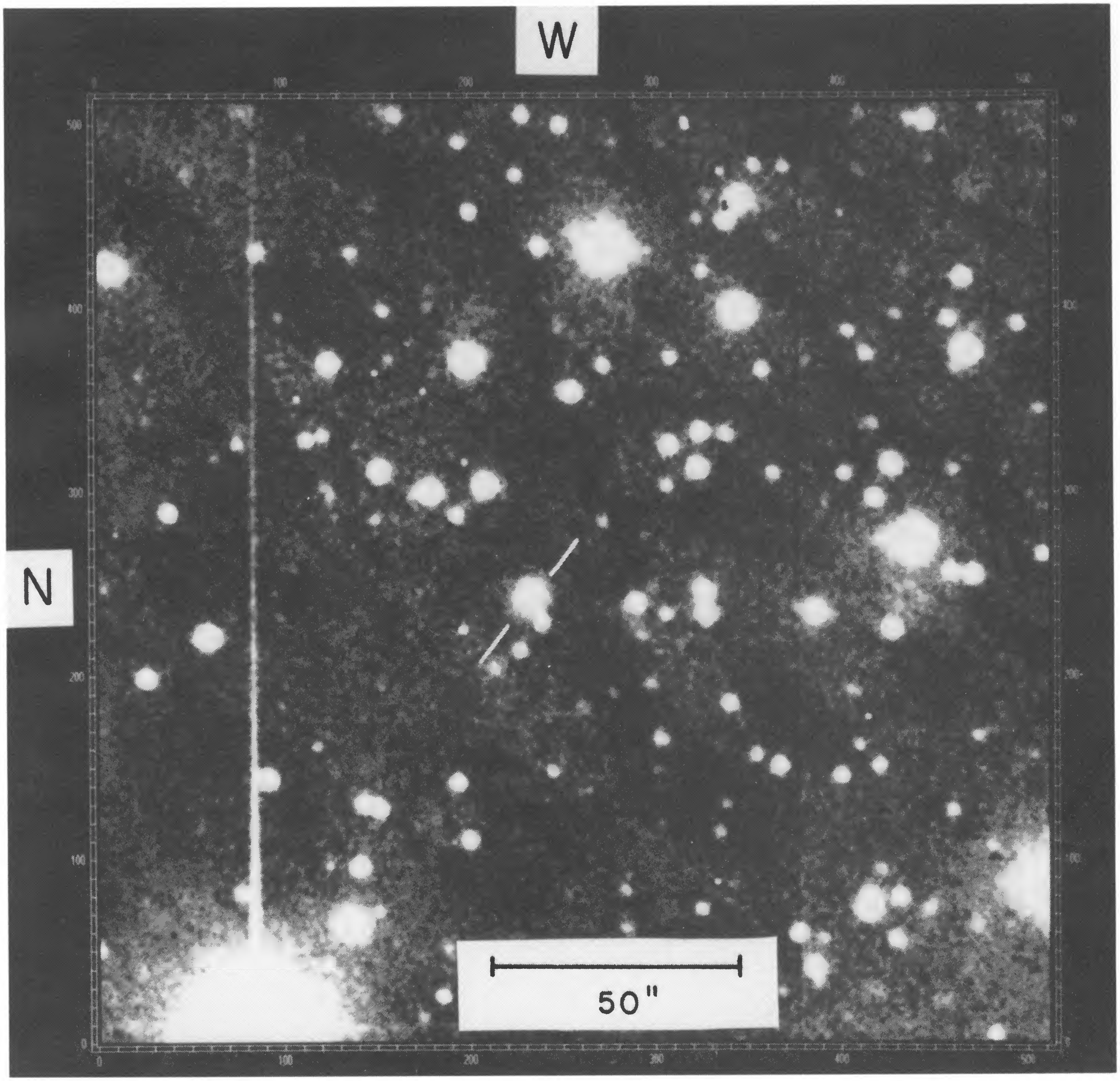

FIG. 1.—The area around IRAS 20460 + 1925 (between the tic marks) as seen on the *I* CCD frame described in the text. The horizontal bar indicates the scale. The mottled appearance is the result of incomplete fringe removal.

FROGEL *et al.* (*see* **343**, 672)

TABLE 1

INFRARED MAGNITUDES AND FLUXES FOR IRAS 20460+1925

Wavelength	Magnitude	log F_ν(Wm^{-2} Hz^{-1})
	Ground-based Data[a]	
J	13.93 ± 0.08	−28.39
H	12.67 ± 0.04	−28.08
K	11.15 ± 0.03	−27.67
L	9.22 ± 0.06	−27.24
M	8.35 ± 0.27	−27.16
[10 μm]	6.78 ± 0.26	−27.14
	IRAS Data[b]	
12 μm	...	−26.62
25 μm	...	−26.22
60 μm	...	−25.99
100 μm	...	−26.1

[a] The data at J, H, K, L, and M were obtained through an aperture of diameter 12″. The 10 μm measurement was obtained through an aperture of diameter 7″.

the smaller aperture. The 10 μm measurement in Table 1 was obtained on 1986 October 20 with a Ga:Ge bolometer on the same telescope with a 6″ diameter aperture. We estimate that the 10 μm flux given in Table 1 may be too low by 20%–30% due to problems in centering the source at this wavelength.

Table 1 also lists *IRAS* measurements for IRAS 20460+1925. These are co-added survey data kindly supplied to us by Dr. C. Beichman. They have been color corrected following the precepts in the *IRAS Explanatory Supplement* (1985). These corrections were not more than 2%. The *IRAS* catalog gives an upper limit at 100 μm while the coadded data give a rather uncertain flux nearly a factor of 2 lower than the upper limit. The large uncertainty arises from the presence of infrared cirrus at the relatively low galactic latitude of the source. We have somewhat arbitrarily assigned a flux at 100 μm half way between the upper limit and the coadded value. Figure 2 displays the data from Table 1 as well as the energy distributions of several other *IRAS* sources. The problems associated with the 10 μm measurement mentioned above may be the origin of the strong dip observed at this wavelength.

b) Optical Spectroscopy

Optical spectroscopy reveals the extragalactic nature of IRAS 20460+1925. Spectra were obtained on 1988 June 1 with the CTIO 4 m telescope, its RC spectrograph, the Air Schmidt camera, and a GEC CCD chip. The 158 line mm^{-1} grating yielded an effective resolution of 11.5 Å. Two grating settings were used to achieve the wavelength coverage displayed in Figure 3. The blue half is the average of two 600 s exposures while the red half is one 600 s exposure. In the 500 Å region of overlap the two halves agreed in flux to 3%. The spectra were flux calibrated with standards from Baldwin and Stone (1984). Standards with the most featureless spectra were used to remove the strongest terrestrial absorption features.

The spectrum of IRAS 20460+1925 is dominated by flux from its bright unresolved nucleus. Broad emission lines from elements in high and low ionization states are present. There are lines of [Fe VII] and [Ar III] along with forbidden lines from neutral N and O. No stellar absorption features are apparent. The presence of NaD and Mg *b* absorption lines cannot be verified as the former lies close to the atmospheric *B* band while the latter is close to [N I] emission. An upper limit to the equivalent width of the Mg *b* line however, is less than 1 Å.

Table 2 lists the observed wavelengths, fluxes, and full width half-maxima (FWHM) of the identified emission lines. Also given in the table are the fluxes with respect to Hβ after correcting for a Galactic reddening of $E(B-V) = 0.10$ (based on the maps in Burstein and Heiles 1982) with the Whitford reddening law as parameterized by Miller and Matthews

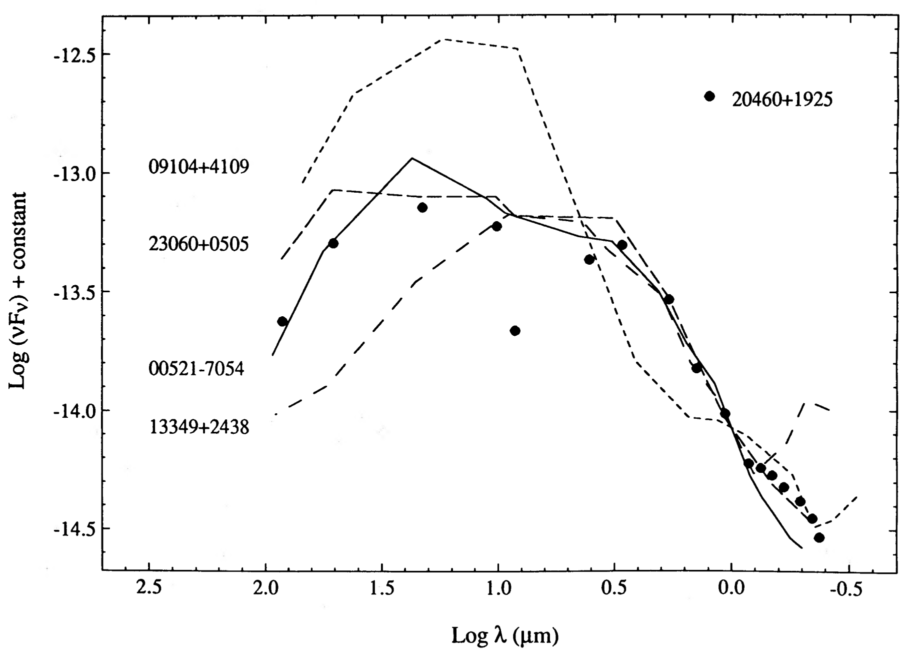

FIG. 2.—The rest frame power spectrum of IRAS 20460+1925 from the data in Table 1 and 2. The optical fluxes have been increased by 0.4 dex to compensate for slit losses. The data for the comparison objects have been normalized at 1 μm in their rest frames.

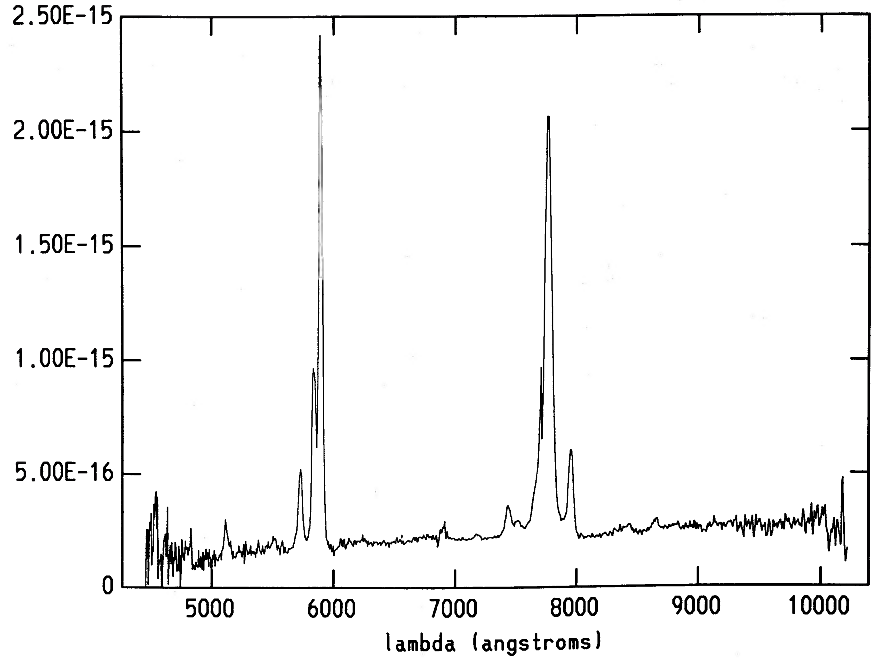

FIG. 3.—A flux calibrated spectrum of IRAS 20460+1925. Units are ergs $cm^{-2} s^{-1}$ Å. The strongest telluric features have been removed.

(1972). The corrected Hβ flux is 1.82×10^{-14} ergs $s^{-1} cm^{-2}$. A redshift of $z = 0.181 \pm 0.001$ is derived from the stronger emission lines. Strengths of the component lines in the strong blends Hα + [N II], [S II], and Hγ + [O III] lines were estimated by fitting Gaussian profiles and are uncertain by 20%–30%. The range in the FWHM of the various lines corresponds to velocities between 1700 and 2100 km s^{-1} in the rest frame. The full width zero intensity (FWZI) of Hβ is ~4300 km s^{-1}. The partial merging of Hα and the [S II] blend is also indicative of a high FWZI.

TABLE 2

A. EMISSION LINES[a]

λ(obs) (Å)	Observed Values			Corrected for $E(B-V) = 0.10$	
	Line	FWHM (Å)	f_λ(obs)	f_λ(corr)	f_λ/f_λ(Hβ)
5131.8.....	Hγ	36.4	43	58	0.32
5159.8.....	[O III]	44	21	28	0.16
5530.0.....	He II	44.4	23	30	0.17
5745.1.....	Hβ	40.0	140	182	1.00
5853.1.....	[O III]	34.2	293	379	2.08
5909.7.....	[O III]	36.7	846	1086	5.97
7445.4.....	[O I]	42.1	57	68	0.37
7733.4.....	[N II]	65	20	23	0.13
7749.7.....	Hα	65	980	1154	6.34
7775.0.....	[N II]	66	510	600	3.30
7935.4.....	[S II]	56.5	133	156	0.85
7953.4.....	[S II]	43.5	106	124	0.68
8426.8.....	[Ar III]	61.2	26	30	0.16
8646.2.....	[O II]	62.4	29	33	0.18

B. CONTINUUM FLUXES

λ(obs) Å	log F_ν(obs)	log F_ν(corr)
5000.......	−29.84	−29.71
6000.......	−29.59	−29.48
7000.......	−29.43	−29.35
8000.......	−29.31	−29.25
9000.......	−29.22	−29.17
10000.......	−29.15	−29.10

[a] In ergs $cm^{-2} s^{-1} \times 10^{16}$.
[b] $Wm^{-2} Hz^{-1}$; fitted with straight line.

According to the classification scheme of Veilleux and Osterbrock (1987) values for the line ratios of [O I], [N II], and [S II] to Hα and the [O III] to Hβ ratio place the galaxy on the boundary between Seyfert 2 galaxies and other types of AGNs such as low-ionization nuclear emission line regions (LINERs) and narrow-line radio galaxies. The width of both forbidden and permitted lines, though, indicates a Sy 2 classifcation for IRAS 20460+1925. Both the FWHM and FWZI of the lines are among the broadest known for a Sy 2. On the whole, its emission-line spectrum is quite similar to that of the much lower luminosity galaxy IRAS 1319−164 studied by De Robertis, Hutchings, and Pitts (1988) except that the latter has stronger [O III], and [N II], and is at a much smaller redshift. Both galaxies also have nearly featureless continua. We note that the large value for the internal reddening derived below will not affect the classification based on Veilleux and Osterbrock's scheme since it is based on ratios of lines with small wavelength separations.

c) Optical Imaging

A 512 square Tektronics CCD chip was used by Dr. R. Probst on 1986 October 24 to obtain 600 s images of IRAS 20460+1925 at V and I with the KPNO No. 1 0.9 m telescope. FWHM profiles for stellar images were 1".8 at V and I. Figure 1 shows a portion of the I frame. On the Kron-Cousins system values measured for IRAS 20460+1925 through an equivalent aperture of diameter 10".8 are $V = 17.65 \pm 0.05$ and $V-I = 2.15 \pm 0.05$. Multiaperture photometry of IRAS 20460+1925 and several stars of similar brightness or redness, or both, show that for the stars 90% of the light at V and I is contained within an aperture of ~5" diameter. IRAS 20460+1925, on the other hand, is considerably extended,

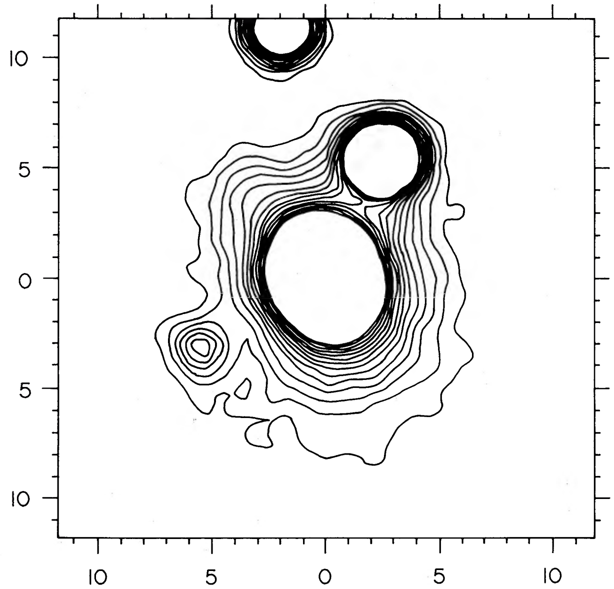

FIG. 4.—A contour plot from a V frame of the immediate vicinity around IRAS 20460+1925. North is to the right, east to the top. Tickmarks are in arc seconds. The seeing resulted in a FWHM = 1".4 for stars. The unresolved cores of the galaxy and the stars have been removed.

more so at V than at I. At V, $\sim$35% of the light is in an extended halo whereas at I the figure is 20%. As noted above, at J, H, and K this extended emission was not detected at all. The point spread function determined for the frames with DAOPHOT (Stetson 1987) was subtracted from the image of IRAS 20460+1925. In a 10".8 aperture we measured $V = 19.1$ and $V-L = 1.8$ for the extended emission, consistent with values determined from the growth curves. For $H_0 = 75$ km s^{-1} Mpc and $q_0 = 0.5$, the diameter of this emission corresponds to 35 kpc and its luminosity is $M_V = -20.3$. This size and magnitude, when corrected for galactic absorption alone, are comparable to values for giant spiral or elliptical galaxies. The total absorption corrected $M_V = -22.3$ of IRAS 20460+1925 is comparable to that for cD galaxies (e.g., Malamuth and Kirshner 1985).

We obtained a deeper 600 s V frame of IRAS 20460+1925 with the CCD system at the prime focus of the CTIO 4 m on 1988 September 9 under somewhat better seeing conditions—FWHM = 1".4—than obtained for the 0.9 m frames. Figure 4 shows a contour plot of IRAS 20460+1925 and the objects in its immediate vicinity. The unresolved core has been eliminated from the *IRAS* object—as have the cores of the stars—to show the faint extended emission. To the upper right of the *IRAS* source is a moderately bright star (as is the object only partially within the frame) also visible in Figure 1. The lowest contour is approximately $\mu = 24$ mag arcsec^{-2}. The very faint wings of IRAS 20460+1925 are decidedly elliptical with an axial ratio of 1.4:1 and can be seen out to a major axis diameter of 13".9. With the possible exception of objects below the threshold set for the DAOPHOT "find" algorithm, we could find no evidence for other extended objects on the CCD frame. Any neighboring galaxy must be at least 3 mag fainter in I than the *IRAS* source—the object to its lower left in Figure 4, for example—or else have a light distribution indistinguishable from the stellar PSF.

III. DISCUSSION

a) Internal Reddening and the Filling Factor

From the observed strengths of the hydrogen recombinations lines we can estimate the reddening internal to IRAS 20460+1925. We make the common assumptions of $T = 10{,}000$ K, $N_e = 10^4$ cm^{-3}, and case B for the Balmer decrement; changes of a factor of 2 in temperature and a factor of 100 in density will not significantly affect the outcome of the calculation (Osterbrock 1974). The Whitford reddening curve, as parameterized by Miller and Mathews (1972), was used. The applicability of its use for galactic nuclei is discussed by Veilleux and Osterbrock (1987). With recombination values for $I(\text{H}\alpha)/I(\text{H}\beta)$ and $I(\text{H}\beta)/I(\text{H}\gamma)$ of 2.85 and 2.13, respectively, we obtain values for A_V of 2.25 and 2.55 mag, respectively, or a mean of $A_V = 2.4$ mag. These two values do not differ by more than expected from the uncertainties in the line fluxes resulting from the strongly blended character of Hα and Hγ. We also note that the intrinsic Balmer decrements for AGNs may be slightly greater than the recombination values (e.g., Gaskell and Ferland 1984; Ward *et al.* 1988).

As discussed below, it is possible that most of the bolometric luminosity of IRAS 20460+1925 is thermal reemission from dust. On the other hand, the fact that the object is quite bright optically implies that the nucleus is not completely masked by the dust. Following the same line of reasoning as Kleinmann *et al.* (1988; see, e.g., Osterbrock 1974) we can estimate what fraction of the central source is visible. This faction is calculated by assuming that the Hβ flux (corrected for A_V of 2.4 mags) is emitted by a region that absorbs all of the incident Lyman continuum photons and that the total Lyman continuum luminosity so calculated should equal the observed bolometric luminosity for the case of no masking. We find that $\sim$5% of the central source is visible.

b) Luminosity

IRAS 20460+1925 is the second most luminous object so far discovered in the *IRAS* survey. The only type of extragalactic objects with several examples significantly more luminous than this source is quasars. Sanders *et al.* (1988*a*, *b*) compute the total luminosity of ultraluminous *IRAS* galaxies by taking 1.8 times the sum of νF_ν for the four *IRAS* bands. The spectral energy distribution of IRAS 20460+1925 is so flat, though, that the calculated luminosity must be corrected upward by 15% to allow for the flux shortward of 8 μm. The resulting luminosity of this remarkable object is log $L = 12.88$ $L_\odot$. The one galaxy known to be more luminous than this, IRAS 09104+4109 (Kleinmann *et al.* 1988), is also a Seyfert 2 but with lines only half as broad as those of IRAS 20460+1925 and with quite a different power spectrum (see, e.g., Fig. 2).

c) Energy Distribution

With the exception of the dip in the 10 μm flux, the energy distribution of IRAS 20460+1925 is quite similar to that of IRAS 00521−7054 (Fig. 2). Both combine exceptionally warm FIR colors with outstandingly red NIR colors. IRAS 20460+1925 has slightly redder *JHKLM* colors while the FIR colors of IRAS 00521−7054 are somewhat warmer with a stronger luminosity peak at 25 μm. Very few other galaxies or quasars have near NIR colors of comparable redness. Three such objects known to us are NGC 5506, a relatively low luminosity Seyfert 2 (J. A. Frogel, J. H. Elias, and M. M. Phillips, unpublished, illustrated in Frogel and Elias 1987), IRAS

23060+0505 (Hill, Wynn-Williams, and Becklin 1987), an active galaxy somewhat less luminous than IRAS 20460+1925, and IRAS 13349+2438, the first quasar discovered by *IRAS* (Beichman *et al.* 1986).[2] The rest frame energy distributions of these objects (except NGC 5506) are compared in Figure 2. They have been normalized to the emission of IRAS 20460+1925 at 1 μm. The optical continuum of the *IRAS* quasar is the only one to exhibit a distinct upturn in the blue (the energy distribution of IRAS 09104+4109 is markedly different from the rest); the other three have red optical continua with slopes quite similar to those of the NIR energy distribution. The FIR colors for all of the objects are at the extreme end of the distribution for Seyfert galaxies and quasars, (Miley, Neugebauer, and Soifer 1985; Neugebauer, Soifer, and Miley 1985; Neugebauer *et al.* 1986).

The close similarity of the energy distributions of IRAS 20460+1925, 00521−7054, 13349+2438, and 23060+0505 suggests a common origin for the infrared emission in these objects. Of particular note is the fact that from 1 to 3 μm the 4 objects are virtually indistinguishable. This seems to imply that a physical process is acting to set a limit to the steepness of this part of the energy distribution. As Frogel and Elias (1987) argued, it is impossible to fit the NIR flux with reddened starlight, and it has too steep a slope to be due to nonthermal power-law emission alone. Hill *et al.* and Frogel and Elias attributed the bulk of the NIR flux in IRAS 20460+1925 and 00521−7054, respectively, to thermal emission from dust. Much earlier, Rieke (1978) argued that " type 1 Seyfert galaxies with *relatively steep infrared spectra* (our italics) emit in the infrared through thermal reradiation by dust." He made a similar argument for Seyfert 2 galaxies.

The steep, nearly continuous slope of the NIR and optical continuum for IRAS 23060+0505, 20460+1925, and 00521−7054 would require, according to the analyses of Malkan and Fillipenko (1983) and Carleton *et al.* (1987), a significant, if not dominant, contribution of direct nonthermal emission (probably reddened) from the central source in the optical and at shorter NIR wavelengths, while hot thermal emission from dust heated by the central source could be important only at wavelengths longer than 2 μm. Barvainis (1987) has demonstrated how graphite grains heated to their evaporation temperature ($\sim$1500 K) can be an important contributor to the NIR emission in active galaxies and quasars. His model closely fits the energy distribution of IRAS 13349+2438 and demonstrates that the dust dominates the emission longward of 2 μm whereas nonthermal power-law emission and flux from a hot blackbody (e.g., the accretion disk) dominate at shorter wavelengths. The source of the graphite grains is a separate question. Minor modifications to this model, for example greater internal reddening or less luminosity in the hot blackbody, or both, would result in good fits to IRAS 20460+1925 and the other objects in Fig. 2. The important point is that Barvainis' model provides a natural explanation for the nearly identical NIR energy distributions: they can be produced by dust heated to its evaporation temperature by the central energy source. This temperature limit naturally results in a limiting shape to the energy distributions.

[2] The second *IRAS*-discovered quasar, IRAS 00275−2859 (Vader *et al.* 1987), has nearly as red NIR colors as these other sources and a somewhat cooler FIR energy distribution. Of the very red QSOs identified with radio sources (e.g., Rieke, Lebofsky, and Wisniewski 1982), the ones with the reddest NIR colors are all variable with sizable amplitudes.

IV. SUMMARY AND CONCLUSIONS

We have shown that IRAS 20460+1925 is associated with a Seyfert 2 galaxy at a redshift of 0.181, a diameter of more than 35 kpc, and an optical luminosity $M_V = -22.3$. Bolometrically it is the second most luminous galaxy (nonquasar) known. The permitted and forbidden lines are broader than those of most other Seyfert 2 galaxies. The presence of a broader still underlying component to the hydrogen lines can be interpreted as evidence for an observed Seyfert 1 nucleus or even a QSO; see, e.g., Antonucci and Miller's analysis of NGC 1068 (1985). Finally, IRAS 20460+1925 does not appear to be associated with a rich cluster of galaxies or to be an interacting system.

The continuous energy distribution from 0.5 to 3.5 μm can be fitted by power laws of the form $f_\nu \propto \nu^{-\alpha}$ with α between 2 and 2.5. The latter value characterizes the NIR wavelengths while the less steep former value provides a better fit to the optical wavelengths. There is no blue turnup although if the optical continuum were dereddened by an amount comparable to that inferred from the Balmer decrement, such a turnup would result. Starlight does not make an observable contribution to the flux from 0.5 to 3.5 μm. Instead, the radiation in this spectral regime can be explained as arising from a combination of nonthermal emission from the central source, hot thermal emission from an accretion disk, and thermal emission from dust grains with a wide range in temperature but with a possibly significant contribution from grains heated by the central source to their evaporation temperature. The FIR energy distribution as determined by *IRAS* is consistent with that of many Seyferts and quasars although the peak at 60 μm places IRAS 20460+1925 at the warm extreme for these objects.

The three *IRAS* galaxies with extreme NIR colors have some striking similarities. Even IRAS 13349+2438, the *IRAS* quasar, has a "narrow" line component with velocity widths nearly identical to those of IRAS 20460+1925; it is also morphologically similar to the latter object in that it consists of an unresolved source surrounded by an extended emission region. The lack of galaxies with redder NIR colors than those exhibited by the objects in Figure 2 suggests that a physical process is acting to set a limit to the shape of the distributions. The models of Barvainis (1987) show that such a limit can arise from the dust grains radiating at or near to their evaporation temperature.

As we will show in a subsequent paper (Vader *et al.* 1989) there are statistically significant correlations, visible both in our sample of IRAS galaxies that peak at 60 μm and in the ultraluminous sample of Sanders *et al.* (1988*a*), between the slope of the NIR energy distribution, the ratio of NIR to FIR luminosities, and the FIR dust temperature in the sense that the less the FIR dominates the total energy output, the steeper the NIR and the hotter is the FIR dust temperature (see Vader *et al.* 1988). Sanders *et al.* noted that an increase in the NIR flux is associated with warmer FIR colors for ultraluminous galaxies and proposed an evolutionary origin for such a correlation. Carico *et al.* (1988) have also argued that the mechanism which produced very red *JHK* colors in galaxies only operates at high luminosity. As Frogel and Elias (1987) pointed out, though, extreme near to far-infrared energy distributions and exceptionally red NIR colors such as are exhibited in their Figure 1 and in Figure 2 here can be matched by objects with intrinsic luminosities several orders of magnitudes less than those of ultraluminous galaxies, so that an evolutionary origin or minimum "turn-on" luminosity for the ecorrelations are not necessarily implied. Rather it seems that similarity in the physical processes that operate in these objects, with variations such as are indicated by the models of Barvainis's (1987), are as important as any evolutionary effects.

We further suggest that the angle at which a galaxy with an active nucleus is viewed, regardless of its luminosity, plays as important a role in its observable characteristics as does the particular evolutionary state of the galaxy. Imagine dust being distributed closely around an active nucleus in a toroidal structure. Viewed from the top, at zero inclination angle, we see into the hole wherein lies the AGN and the hot inner parts of the dust distribution. Radiation from these two components will dominate whatever starlight there is. Objects for which the inclination angle may be smaller than that for IRAS 20460+1925, such as the infrared loud quasar (Beichman *et al.* 1986), would exhibit a prominent blue optical continuum as well as a stronger broad-line component in Hα. As our line of sight approaches the plane of the torus, the inner part of the nucleus becomes more and more obscured from sight, and we can see only line emitting regions that lie at increasingly greater distances from the nucleus. The obscuration may become great enough so that the hot dust emission itself is absorbed allowing the FIR emission to dominate. With the NIR and optical emission from the nuclear regions suppressed, starlight from regions of the galaxy outside of the center should become visible. An example would be IRAS 09104+4109 (Kleinmann *et al.* 1988): note its energy distribution in Figure 2, the fact that Kleinmann *et al.* detect the K line of Ca II in absorption, and that they find a covering factor of 98% for the central source, significantly greater than we have calculated for IRAS 20460+1925. The bolometric luminosity of the galaxy would act mainly as a scaling factor determining the nature of the AGN, e.g., the mass and fueling rate of the central black hole.

To separate the effects of evolution from those of geometry is difficult. While morphology may hold a clue in the cases where the nuclear activity is caused by mergers and interactions (see Sanders *et al.* 1987*a*, *b*), it would be premature to attribute all such activity to this cause. Furthermore, it seems reasonable to assume that the dust distribution is going to be strongly time dependent because of the destruction of the grains. As grains are destroyed and the central hole is enlarged, the NIR flux will decrease absolutely while the AGN will shine through more and more brightly. Osterbrock and Shaw (1988) have discussed how the relative number of Seyfert 1 and 2 galaxies can be used to estimate the relative lifetimes of each class if they are stages in an evolutionary sequence, or to estimate the size of the obscuring torus if they are examples of an evolutionary sequence. Further considerations of these ideas and specific observational tests of the various interpretations will be given in Vader *et al.* (1989).

We thank Ron Probst for obtaining the 0.9 m CCD frames for us; Chas Beichman for providing the co-added *IRAS* data; Tom Soifer for information on how he and his collaborators calculated their luminosities; and George Jacoby and Phil Massey for advice on the optical data reduction. This research has been supported in part by NASA grant JPL 958027 to J. P. V.

REFERENCES

Antonucci, R. R. J., and Miller, J. S. 1985, *Ap. J.*, **297**, 621.
Baldwin, J. A., and Stone, R. P. S. 1984, *M.N.R.A.S.*, **206**, 241.
Barvainis, R. 1987, *Ap. J.*, **320**, 537.
Beichman, C. A., Soifer, B. T., Helou, G., Chester, T. J., Gillett, F. C., Low, F. J., and Neugebauer, G. 1986, *Ap. J.* (*Letters*), **308**, L1.
Burstein, D., and Heiles, C. 1982, *A.J.*, **87**, 1165.
Carleton, N. P., Elvis, M., Fabbiano, G., Willner, S. P., Lawrence, A., and Ward, M. 1987, *Ap. J.*, **318**, 595.
Carico, D. P., Sanders, D. B., Soifer, B. T., Elias, J. H., Matthews, K., and Neugebauer, G. 1988, *A.J.*, **95**, 356.
de Grijp, M. H. K., Miley, G. K., Lub, J., and de Jong, T. 1985, *Nature*, **314**, 240.
De Robertis, M. M., Hutchings, J. B., and Pitts, R. E. 1988, *A.J.*, **95**, 1371.
Elias, J. H., Frogel, J. A., Matthews, K., and Neugebauer, G. 1982, *A.J.*, **87**, 1029.
Frogel, J. A., and Elias, J. H. 1987, *Ap. J.* (*Letters*), **313**, L53.
Gaskell, C. M., and Ferland, G. J. 1984, *Pub. A.S.P.*, **96**, 393.
Hill, G. J., Wynn-Williams, C. G., and Becklin, E. E. 1987, *Ap. J.* (*Letters*), **316**, L11.
IRAS Catalogs and Atlases Explanatory Supplement. 1985, ed. C. A. Beichman, G. Neugebauer, H. J. Habing, P. E. Clegg, and T. J. Chester (Washington, DC: US GPO).
Kleinmann, S. G., Hamilton, D., Keel, W. C., Wynn-Williams, C. G., Eales, S. A., Becklin, E. E., and Kuntz, K. D. 1988, *Ap. J.*, **328**, 161.
Malamuth, E. M., and Kirshner, R. P. 1985, *Ap. J.*, **291**, 8.
Malkan, M. A., and Fillipenko, A. V. 1983, *Ap. J.*, **275**, 477.
Miley, G. K., Neugebauer, G., and Soifer, B. T. 1985, *Ap. J.* (*Letters*), **293**, L11.
Miller, J. S., and Mathews, W. G. 1972, *Ap. J.*, **172**, 593.
Neugebauer, G., Miley, G. K., Soifer, B. T., and Clegg, P. E. 1986, *Ap. J.*, **308**, 815.
Neugebauer, G., Soifer, B. T., and Miley, G. K. 1985, *Ap. J.* (*Letters*), **295**, L27.
Osterbrock, D. E. 1974, *Astrophysics of Gaseous Nebulae* (San Francisco: Freeman).
Osterbrock, D. E., and Shaw, R. A. 1988, *Ap. J.*, **327**, 89.
Rieke, G. H. 1978, *Ap. J.*, **226**, 550.
Rieke, G. H., Lebofsky, M. J., and Wisniewski, W. Z. 1982, *Ap. J.*, **263**, 73.
Sanders, D. B., Soifer, B. T., Elias, J. H., Madore, B. F., Matthews, K. Neugebauer, G., and Scoville, N. Z. 1988*a*, *Ap. J.*, **325**, 74.
Sanders, D. B., Soifer, B. T., Elias, J. H., Neugebauer, G., and Matthews, K. 1988*b*, *Ap. J.* (*Letters*), **328**, L35.
Stetson, P. B. 1987, *Pub. A.S.P.*, **99**, 191.
Vader, J. P., Da Costa, G. S., Frogel, J. A., Heisler, C. A., and Simon, M. 1987, *A.J.*, **94**, 847.
Vader, J. P., Frogel, J. A., Gillett, F. C., and de Grijp, M. H. K. 1988, paper presented at the Lick Conference on Active Galaxies.
Vader, J. P., Frogel, J. A., Gillett, F. C., and Terndrup, D. M. 1989, in preparation.
Veilleux, S., and Osterbrock, D. E. 1987, *Ap. J. Suppl.*, **63**, 295.
Ward, M. J., Done, C., Fabian, A. C., Tennant, A. F., and Shafer, R. A. 1988, *Ap. J.*, **324**, 767.

JAY A. FROGEL: Ohio State University, Department of Astronomy, 174 West 18th Avenue, Columbus, OH 43210

DONALD M. TERNDRUP: Cerro Tololo Inter-American Observatory, Casilla 603, La Serena, Chile

J. PATRICIA VADER: Department of Astronomy, Yale University, Box 6666, New Haven, Connecticutt 06511